Elastic quantum transport through small structures

T N Todorov, G A D Briggs and A P Sutton

Department of Materials, University of Oxford, Parks Road, Oxford OX1 3PH, UK

Abstract. We develop a general formulation of the problem of elastic transport between two semi-infinite systems, connected by a system of finite size, and derive expressions for the current in and the differential conductance of such a circuit in the limit of zero interactions between the carriers. These expressions are exact in the applied voltage, the coupling of the components of the circuit, and the temperature of the circuit. We then apply our results in a tight-binding approximation to three specific cases: the one-atom contact, the finite, disordered one-dimensional chain, and the generalized stacking fault.

1. Introduction

In this paper we treat the general problem of elastic quantum transport across a system of finite size placed between two semi-infinite systems. The problem of direct transport between two semi-infinite systems is a subcase of this general problem. The formal essence of the method, developed below, is simple. We start with an initial Hamiltonian, H_0. We divide its complete orthonormal set of eigenstates into two or more mutually orthogonal subsets, each of which bears a clear spatial relation to a particular component of the system described by H_0. Now we add to H_0 a term V that couples these subsets. Finally, we consider the current between the mutually orthogonal subsets of the complete set of eigenstates of H_0 due to some particular filling of the eigenstates of the *final* Hamiltonian, $H = H_0 + V$.

The derivations in sections 2 and 3 are performed from the point of view of an *orthonormal tight-binding model*. At the end of section 3, however, there is a complete description of the implementation of the method in the continuum $|r\rangle$ representation, where $|r\rangle$ is the Dirac ket representing position.

2. The zero-current theorem

The whole of our analysis will rely on one fundamental result, which we prove in this section.

Consider two semi-infinite systems, 1 and 2. The coupling between them is zero (figure 1). In the orthonormal tight-binding picture, employed here, this means that all hopping integrals between the two systems have been set equal to zero.

Let this situation be described by a Hamiltonian H_0. Let system 1 have a continuous set of single-particle eigenstates $\{|\phi_1\rangle\}$ with eigenvalues $\{E_1\}$ and system 2 have a continuous set of single-particle eigenstates $\{|\phi_2\rangle\}$ with eigenvalues $\{E_2\}$. The set of vectors $\{|\phi_n\rangle\}$,

Figure 1. Two uncoupled semi-infinite systems, 1 and 2.

where n runs over all possible values of indices 1 and 2, is the set of eigenvectors of H_0; $\{|\phi_n\rangle\}$ is a complete orthonormal set. The sets $\{|\phi_1\rangle\}$ and $\{|\phi_2\rangle\}$ are two mutually orthogonal subsets of the complete set of eigenstates of H_0, such as those discussed in the introduction. Let $G^{0\pm}$ be the Green operators for the initial, decoupled system

$$G^{0\pm}(E) = \lim_{\epsilon \to 0^+} (E - H_0 \pm i\epsilon)^{-1}. \tag{1}$$

The density-of-states operator, ρ^0, for the initial system is given by

$$\rho^0(E) = [G^{0-}(E) - G^{0+}(E)]/(2\pi i). \tag{2}$$

From equations (1) and (2) we obtain

$$\rho^0(E)|\phi_n\rangle = \delta(E - E_n)|\phi_n\rangle. \tag{3}$$

Now we couple systems 1 and 2 by an additive term V in the Hamiltonian. Thus, the new Hamiltonian H is given by

$$H = H_0 + V. \tag{4}$$

V represents the switching on of the hopping between systems 1 and 2 but may have other non-zero matrix elements too. We assume that V causes no level shifts, i.e. that the eigenstates of H (which we assume to be single-particle states) also form a continuum in such a way that to every eigenstate of H_0 there corresponds exactly one eigenstate of H with the same energy. At this stage of the argument, we encounter a subtlety, which we must discuss in order to avoid confusion. So far we have ignored particle interactions inasmuch as we have chosen to work with single-particle states as opposed to antisymmetrized many-particle states. However, we may not neglect self-consistency altogether, even at this level of simplicity, owing to the absolutely uncompromisable requirement that, both before and after the coupling V has been introduced, systems 1 and 2 have to be electrically neutral. This requirement means that we cannot divorce the act of coupling 1 and 2 from the act of filling the new eigenstates with electrons. In particular, with every mode of filling of these eigenstates will be associated a rigid energy shift of the whole of 2 relative to 1, to satisfy the neutrality condition. (For example, the contact potential is the rigid energy shift associated with the equilibrium filling of the eigenstates for two coupled dissimilar metals, and the battery voltage, to be discussed later, is the rigid energy shift associated with a particular non-equilibrium filling of the eigenstates for the coupled system.) Now, what we actually do is decide what mode of filling of the eigenstates for the coupled system we are going to adopt, determine the associated rigid shift of the potential of 2 relative to that of 1, *and include that shift in H_0.* Thus we know that, so long as we do adopt the mode of filling of the eigenstates for the coupled system for which that energy shift was chosen, the assumption of 'no level shifts', mentioned earlier, will hold.

We have assumed that H_0 and H have no bound states, but all results will hold when H_0 or H, or both, do have bound states, so long as these bound states lie outside the respective continua.

The eigenstates of H, $\{|\psi_n^+\rangle\}$, satisfy the Lippmann–Schwinger equation

$$|\psi_n^+\rangle = |\phi_n\rangle + G^{0+}(E_n)V|\psi_n^+\rangle \tag{5}$$

where E_n is the energy of $|\phi_n\rangle$ and $|\psi_n^+\rangle$. $\{|\psi_n^+\rangle\}$ is a complete orthonormal set. The Green operators $G^{\pm}$ for the coupled system are given by

$$G^{\pm}(E) = \lim_{\epsilon \to 0^+} (E - H \pm i\epsilon)^{-1}. \tag{6}$$

The density-of-states operator, ρ, for the coupled system is given by

$$\rho(E) = [G^-(E) - G^+(E)]/(2\pi i). \tag{7}$$

Therefore

$$\rho(E)|\psi_n^+\rangle = \delta(E - E_n)|\psi_n^+\rangle. \tag{8}$$

Now we derive an expression for the operator representing the current in the system. This is the operator for the current *into* system 2, i.e. for the current into the set of states $\{|\phi_2\rangle\}$. The operator for the current into any state $|u\rangle$, I_u, is given by

$$I_u = (e/i\hbar)(|u\rangle\langle u|H - H|u\rangle\langle u|). \tag{9}$$

This result follows from the Schrödinger equation of motion for the operator $|u\rangle\langle u|$.

Hence, the operator for the current into system 2, I, is given by

$$I = \frac{e}{i\hbar} \sum_2 (|\phi_2\rangle\langle\phi_2|H - H|\phi_2\rangle\langle\phi_2|). \tag{10}$$

But since $|\phi_2\rangle\langle\phi_2|H_0 = |\phi_2\rangle E_2\langle\phi_2| = H_0|\phi_2\rangle\langle\phi_2|$, equation (10) becomes

$$I = \frac{e}{i\hbar} \sum_2 (|\phi_2\rangle\langle\phi_2|V - V|\phi_2\rangle\langle\phi_2|). \tag{11}$$

The fundamental result, or 'the zero-current theorem', which we have set out to prove, is the following: *the sum of the expectation values of I in all states $|\psi_n^+\rangle$, whose energies E_n lie in an energy interval dE about an energy E, is zero for any E.* The physical meaning of this statement is that, if all states $|\psi_n^+\rangle$ with E_n in $[E, E + dE]$ are equally filled, then the current from 1 into 2 will be cancelled exactly by the current from 2 into 1. Here is the proof:

The sum of the expectation values of I in all states $|\psi_n^+\rangle$ with E_n in $[E, E + dE]$, $dI(E)$, is given by

$$dI(E) = dE \, \mathrm{Tr}[I \rho(E)]. \tag{12}$$

Taking the trace in the orthonormal basis $\{|\psi_n^+\rangle\}$, we obtain

$$dI(E) = \frac{e \, dE}{\hbar} \frac{1}{i} \sum_{n;2} \left(\langle\psi_n^+ | \phi_2\rangle\langle\phi_2|V|\psi_n^+\rangle - \langle\psi_n^+|V|\phi_2\rangle\langle\phi_2 | \psi_n^+\rangle \right) \delta(E - E_n). \tag{13}$$

But, by definition, $\langle\phi_2|V|\psi_n^+\rangle = \langle\phi_2|T|\phi_n\rangle \equiv T_{2n}$, where T is the T-operator, and from equations (5) and (1), $\langle\phi_2 | \psi_n^+\rangle = \delta_{2n} + G^{0+}(E_n)_{22}T_{2n}$. (Throughout the present section, M_{pq} will be understood to mean $\langle\phi_p|M|\phi_q\rangle$, for any operator M.) Therefore, equation (13) becomes

$$dI(E) = \frac{e \, dE}{\hbar} \frac{1}{i} \sum_{2;n} \left\{ [\delta_{2n} + G^{0+*}(E_n)_{22}T_{2n}^*]T_{2n} - [\delta_{2n} + G^{0+}(E_n)_{22}T_{2n}]T_{2n}^* \right\} \delta(E - E_n). \tag{14}$$

But since $G^{0+\dagger} = G^{0-}$ and $G^{0-}(E_n)_{22} - G^{0+}(E_n)_{22} = 2\pi i \rho^0(E_n)_{22} = 2\pi i \delta(E_n - E_2)$, equation (14) becomes

$$dI(E) = \frac{edE}{\hbar} \sum_2 \left(\frac{(T_{22} - T_{22}^\dagger)}{i} \delta(E - E_2) + 2\pi \sum_n |T_{2n}|^2 \delta(E_n - E_2) \delta(E - E_n) \right). \quad (15)$$

However, as a consequence of the unitarity condition $(SS^\dagger)_{pq} = \delta_{pq}$, where S is the S-matrix, defined by $S = \Omega^{-\dagger}\Omega^+$, with $\Omega^\pm$ being the Møller operators, defined by

$$\Omega^\pm = \sum_m |\psi_m^\pm\rangle\langle\phi_m|$$

and of the relation $S_{ab} = \delta_{ab} - 2\pi i \delta(E_a - E_b)T_{ab}$, the matrix elements of T satisfy the well known relation (see e.g. [1])

$$T_{pq} - T_{pq}^\dagger = -2\pi i \sum_n T_{pn}T_{qn}^* \delta(E_n - E_p) \qquad \text{for } E_p = E_q. \quad (16)$$

Putting $p = q = 2$ and substituting in (15), we finally obtain

$$dI(E) = \frac{edE}{\hbar} \sum_2 \left(-2\pi \sum_n |T_{2n}|^2 \delta(E_n - E_2)\delta(E - E_2) \right.$$

$$\left. + 2\pi \sum_n |T_{2n}|^2 \delta(E_n - E_2)\delta(E - E_n) \right) = 0 \quad (17)$$

which is the result we wished to prove.

3. Derivation of the current and conductance formulae

We now turn to our main task—the discussion of elastic transport through small structures. The term 'small structure' will be employed somewhat loosely to designate any structure whose linear dimension in the direction of current flow is small compared with the inelastic mean free path of the carriers in the bulk of the respective substance. A small structure will therefore act as a predominantly elastic scatterer. We confine our analysis to the limit when the small structure under study, as well as all other components of the circuit, of which it is a part, acts as a purely elastic scatterer. Also, we shall work with single-particle states, assuming non-interacting carriers. (Self-consistency corrections can in principle be introduced into the analysis, but this possibility will not be dealt with in this work.)

The above-defined conduction regime leads to a simple picture of the conducting circuit. In this picture, the small structure, which from now on will be referred to as the 'sample', is connected by semi-infinite (not necessarily perfectly conducting, but, necessarily for this analysis, elastically scattering) leads to a system of heat-particle reservoirs, where all inelastic scattering takes place and thermal equilibrium reigns.

In the case of two reservoirs, the configuration represents an ordinary battery, connected across the sample. The difference between the absolute positions of the Fermi levels of the two reservoirs is the battery voltage. (The absolute position of the Fermi level is known as the electrochemical potential, as opposed to the position of the Fermi level relative to some reference core state, which is known as the chemical potential.) The current is due to the unequal filling of the right- and the left-going eigenstates of the lead–sample–lead system.

We now consider the three-component system, described above, as represented schematically in figure 2. The two semi-infinite systems 1 and 2 are the leads and the

finite system s is the sample. The three components are decoupled (which, once again, in the orthonormal tight-binding picture employed here, means that all hopping integrals between the components are zero), and the potential energy of the whole of 2 has been adjusted so that the electrochemical potential of 2 lies an amount eW below that of 1, where W will be the battery voltage. In the light of our previous discussion, we include in H_0 a rigid shift of the potential of 2 relative to that of 1 in such a way that both 1 and 2 will be electrically neutral when we fill the eigenstates of the coupled lead–sample–lead system with the non-equilibrium distribution, provided by the battery. Let system 1 have a continuous set of single-particle eigenstates $\{|\phi_1\rangle\}$ with eigenvalues $\{E_1\}$ and system 2 have a continuous set of single-particle eigenstates $\{|\phi_2\rangle\}$ with eigenvalues $\{E_2\}$. Let s have a discrete set of single-particle eigenstates $\{|\phi_s\rangle\}$ with eigenvalues $\{E_s\}$. Thus, the union of the vector sets $\{|\phi_n\rangle\}$, where n runs over all possible values of indices 1 and 2, and $\{|\phi_s\rangle\}$ is the set of eigenvectors of the initial Hamiltonian, H_0. $[\{|\phi_n\rangle\}, \{|\phi_s\rangle\}]$ is a complete orthonormal set. The sets $\{|\phi_1\rangle\}$, $\{|\phi_2\rangle\}$ and $\{|\phi_s\rangle\}$ are three mutually orthogonal subsets of the complete set of eigenstates of H_0, such as the ones discussed in the introduction.

Figure 2. The uncoupled three-component system: the semi-infinite systems 1 and 2 are the leads, and the finite system s is the sample.

We define the Green operators $G^{0\pm}$ and the density-of-states operator ρ^0 for the initial, decoupled system as before, by equations (1) and (2), respectively. This time, however, we note that we can write $G^{0\pm}(E)$ as

$$G^{0\pm}(E) = \lim_{\epsilon \to 0^+} \sum_{1;s;2} \left(\frac{|\phi_1\rangle\langle\phi_1|}{E - E_1 \pm i\epsilon} + \frac{|\phi_s\rangle\langle\phi_s|}{E - E_s \pm i\epsilon} + \frac{|\phi_2\rangle\langle\phi_2|}{E - E_2 \pm i\epsilon} \right). \quad (18)$$

Now we define two projection operators, P_1 and P_2, as follows

$$P_1 = \sum_1 |\phi_1\rangle\langle\phi_1| \quad (19)$$

$$P_2 = \sum_2 |\phi_2\rangle\langle\phi_2| \quad (20)$$

and observe that

$$P_1 G^{0\pm}(E) = G^{0\pm}(E) P_1 = \lim_{\epsilon \to 0^+} \sum_1 \frac{|\phi_1\rangle\langle\phi_1|}{E - E_1 \pm i\epsilon} = G_1^{0\pm}(E) \quad (21)$$

where $G_1^{0\pm}$ are the Green operators for system 1 only. Similarly

$$P_2 G^{0\pm}(E) = G^{0\pm}(E) P_2 = G_2^{0\pm}(E) \quad (22)$$

where $G_2^{0\pm}$ are the Green operators for system 2 only. We also have

$$P_1 \rho^0(E) = \rho^0(E) P_1 = \rho_1^0(E) \quad (23)$$

and

$$P_2 \rho^0(E) = \rho^0(E) P_2 = \rho_2^0(E) \quad (24)$$

where ρ_1^0 and ρ_2^0 are the density-of-states operators for systems 1 and 2, respectively.

Now we couple the three systems, 1, s and 2, by an additive term V in the Hamiltonian so that the new Hamiltonian H is $(H_0 + V)$, as in equation (4). Once again, V represents the switching on of the hopping between the three systems, but may in general have other non-zero matrix elements, such as on-site energy shifts, etc.

Again, we assume that V causes no level shifts, so that the eigenstates of H (which we assume to be single-particle states) form a continuum in such a way that to every eigenstate from the continuous part of the spectrum of H_0 there corresponds exactly one eigenstate of H with the same energy. We have assumed that there are no bound states among the eigenstates of systems 1 and 2, or among the eigenstates of H, but, again, all results will also hold when such bound states exist, so long as they lie outside the respective continua.

As before, the eigenstates of H, $\{|\psi_n^+\rangle\}$, arise from the continuum eigenstates of H_0, $\{|\phi_n\rangle\}$, via the Lippmann–Schwinger equation (5), which may equivalently be written as

$$|\psi_n^+\rangle = [1 + G^+(E_n)V]|\phi_n\rangle \tag{25}$$

where G^+ is the Green operator for the coupled system. (The Green operators $G^\pm$ and the density-of-states operator ρ for the coupled system are defined as before, by equations (6) and (7), respectively.) $\{|\psi_n^+\rangle\}$ is a complete orthonormal set. Note that via the energy shift eW in H_0, both $G^{0\pm}(E)$ and $G^\pm(E)$ are implicitly functions of W.

We shall find it convenient to divide the set of states $\{|\psi_n^+\rangle\}$ into two subsets: one of them is $\{|\psi_1^+\rangle\}$, the eigenstates of H that have come from the states $\{|\phi_1\rangle\}$, and the other one is $\{|\psi_2^+\rangle\}$, the eigenstates of H that have come from the states $\{|\phi_2\rangle\}$. The states $\{|\psi_1^+\rangle\}$ are travelling to the right, and the states $\{|\psi_2^+\rangle\}$ to the left.

For the current operator, I, for the coupled system we once again choose the operator that represents current *into* system 2. I is given by equation (10), which reduces to equation (11) as before. Now we write (11) as

$$I = (e/i\hbar)(P_2 V - V P_2) \tag{26}$$

where P_2 is the projection operator defined in (20). Our task this time is to calculate $dI_R(E)$, the sum of the expectation values of I in all *right-moving* eigenstates of the coupled system with energies in the interval $[E, E + dE]$. Since the right-moving states are the $|\psi_1^+\rangle$, $dI_R(E)$ is given by

$$dI_R(E) = dE \sum_1 \langle \psi_1^+ | I \rho(E) | \psi_1^+ \rangle = \frac{edE}{i\hbar} \sum_1 (\langle \psi_1^+ | P_2 V | \psi_1^+ \rangle$$

$$- \langle \psi_1^+ | V P_2 | \psi_1^+ \rangle) \langle \psi_1^+ | \rho(E) | \psi_1^+ \rangle. \tag{27}$$

We now require the obvious result

$$\langle \psi_1^+ | \rho(E) | \psi_1^+ \rangle = \langle \phi_1 | \rho^0(E) | \phi_1 \rangle \tag{28}$$

which can be proved with ease. Also, from equations (5) and (22)

$$P_2 | \psi_1^+ \rangle = G_2^{0+}(E_1) V | \psi_1^+ \rangle \tag{29}$$

and from (25)

$$V | \psi_1^+ \rangle = t(E_1) | \phi_1 \rangle \tag{30}$$

where $t(E)$ is defined by

$$t(E) = V + V G^+(E) V. \tag{31}$$

Remembering that $G_2^{0+\dagger} = G_2^{0-}$ and that $G_2^{0-}(E) - G_2^{0+}(E) = 2\pi i \rho_2^0(E)$, equation (27) becomes

$$dI_R(E) = dE \frac{2\pi e}{\hbar} \sum_1 \langle \phi_1 | \rho^0(E) | \phi_1 \rangle \langle \phi_1 | t^\dagger(E_1) \rho_2^0(E_1) t(E_1) | \phi_1 \rangle. \tag{32}$$

Owing to the term $\langle \phi_1 | \rho^0(E) | \phi_1 \rangle$ (which vanishes identically unless $E_1 = E$), we can replace E_1 by E everywhere in (32). Also, since ρ^0 is diagonal in $\{|\phi_n\rangle\}$, we can rewrite (32) as

$$dI_R(E) = dE \frac{2\pi e}{\hbar} \sum_1 \langle \phi_1 | \rho^0(E) \left(|\phi_1\rangle\langle\phi_1| + \sum_{1' \neq 1} |\phi_{1'}\rangle\langle\phi_{1'}| \right) t^\dagger(E) \rho_2^0(E) t(E) | \phi_1 \rangle$$

$$= dE \frac{2\pi e}{\hbar} \sum_1 \langle \phi_1 | \rho^0(E) P_1 t^\dagger(E) \rho_2^0(E) t(E) | \phi_1 \rangle. \tag{33}$$

Owing to (23), equation (33) becomes

$$dI_R(E) = dE \frac{2\pi e}{\hbar} \sum_1 \langle \phi_1 | \rho_1^0(E) t^\dagger(E) \rho_2^0(E) t(E) | \phi_1 \rangle. \tag{34}$$

Using the fact that $\rho_1^0 | \phi_2 \rangle = \rho_1^0 | \phi_s \rangle = 0$, for all 2, s, we may rewrite (34) as

$$dI_R(E) = dE \frac{2\pi e}{\hbar} \sum_{k=1;s;2} \langle \phi_k | \rho_1^0(E) t^\dagger(E) \rho_2^0(E) t(E) | \phi_k \rangle. \tag{35}$$

Finally, from (35) we obtain

$$dI_R(E) = dE \frac{2\pi e}{\hbar} \mathrm{Tr}[\rho_1^0(E) t^\dagger(E) \rho_2^0(E) t(E)]. \tag{36}$$

By the zero-current theorem, equation (17), $dI_R(E)$ is exactly equal in magnitude to $dI_L(E)$, the sum of the expectation values of I in all left-moving eigenstates for the coupled system with energies in the interval $[E, E + dE]$. (To see that (17) still holds, imagine only coupling s and one of the leads first, thereby re-creating the starting point of the analysis leading to (17), and then repeating that analysis.) Now we fill the right-going states, $\{|\psi_1^+\rangle\}$, with a Fermi–Dirac distribution $f(E)$, and the left-going states, $\{|\psi_2^+\rangle\}$, with a Fermi–Dirac distribution $f(E + eW)$. The total current I in the system is

$$I = \int [dI_R(E) f(E) - |dI_L(E)| f(E + eW)]$$

$$= \frac{2\pi e}{\hbar} \int \mathrm{Tr}[\rho_1^0(E) t^\dagger(E) \rho_2^0(E) t(E)][f(E) - f(E + eW)] \, dE. \tag{37}$$

Equation (37) is the most general expression for the current across the sample at an applied battery voltage of W, which is exact in W (via the W dependence of $G^{0\pm}(E)$ and $G^{\pm}(E)$), the coupling V and the temperature, within the limits of the conduction regime, specified earlier (which, once again, assumes purely elastic scattering in all parts of the circuit, and single-particle states).

As was stated earlier, the above derivation of (37) is based on an orthonormal tight-binding picture. At the same time, the idea, outlined in the introduction, is perfectly general. For the sake of illustrating its generality, and for the sake of completeness, we shall now discuss briefly the implementation of this idea in the continuum $|r\rangle$ representation.

In this discussion, we shall regard the sample as being a part of one of the leads. Thus, the set-up we envisage corresponds to figure 1 with systems 1 and 2 being two semi-infinite solids, separated by a gap. Let $C(x, y, z) = 0$ define an *open* surface lying *between* systems 1 and 2. Consider the potential barrier given by $\alpha\delta(C)$, where α is a parameter and δ is the Dirac delta function. Let the initial Hamiltonian H_0 include this barrier with some *finite* α. The eigenstates of H_0 fall into two classes: right-moving ones and left-moving ones. The right-moving ones consist of a wave incident in system 1, partially reflected back into 1 and partially transmitted into 2. Conversely, the left-moving ones consist of a wave, incident in system 2, partially reflected back into 2 and partially transmitted into 1. Let the right-moving eigenstates of H_0 be the set $\{|\phi_1\rangle\}$ and the left-moving ones be the set $\{|\phi_2\rangle\}$. Exactly as before, $\{|\phi_1\rangle\}$ and $\{|\phi_2\rangle\}$ are mutually orthogonal and their union, the set of eigenstates of H_0, $\{|\phi_n\rangle\}$, $n = 1, 2$, is complete. Let the coupling V, introduced before, correspond to the *removal* of the barrier $\alpha\delta(C)$, so that the final Hamiltonian, $H = H_0 + V$, describes the fully coupled system. We can now repeat every single step of the derivation presented above and thus calculate the transport between $\{|\phi_1\rangle\}$ and $\{|\phi_2\rangle\}$ due to some filling of the eigenstates of H. All results are going to be implicit functions of the parameter α. In the limit $\alpha \to \infty$, when the initial barrier becomes impenetrable and the transmitted parts of $\{|\phi_1\rangle\}$ and $\{|\phi_2\rangle\}$ become equal to zero, the transport between the two sets of states $\{|\phi_1\rangle\}$ and $\{|\phi_2\rangle\}$ becomes equal to the transport between the two spatial regions, represented by systems 1 and 2. In this limit, equation (37) coincides with the result of the recent time-independent study by Pendry *et al* [2].

Equation (37) is also in agreement with the results of a very recent time-dependent calculation [3], in which the coupling V is switched on adiabatically, and the system is allowed to reach a steady state.

Before carrying on with our main discussion, we shall compare the present formalism with the well known Bardeen transfer Hamiltonian formalism [4] (BTHF). The BTHF is a *first-order time-dependent* perturbation calculation in the continuum $|r\rangle$ representation of the current between two weakly coupled semi-infinite metals 1 and 2 and is based on a very different starting point from one employed in this paper. The essence of the BTHF is the following. Let $\{|\Lambda_1\rangle\}$ be the set of eigenstates of metal 1 *in the absence of metal 2* and $\{|\Lambda_2\rangle\}$ be the set of eigenstates of metal 2 *in the absence of metal 1*. Thus, $\{|\Lambda_1\rangle\}$ and $\{|\Lambda_2\rangle\}$ are both complete and therefore not mutually orthogonal. (Note the difference from the sets $\{|\phi_1\rangle\}$ and $\{|\phi_2\rangle\}$.) An electron is released from a state $|\Lambda_1\rangle$. Its time-evolved state vector is then expressed in terms of the complete set $\{|\Lambda_2\rangle\}$ and the transition rate into each state $|\Lambda_2\rangle$ is computed to *first order* in the hopping integral between $|\Lambda_1\rangle$ and $|\Lambda_2\rangle$. Thus, the BTHF can only be used in the weak-coupling limit. We now return to our main discussion.

Differentiating (37) with respect to the battery voltage W yields the differential conductance of the circuit, G, which is a function of W itself and of the temperature, θ

$$
G(W, \theta) = \frac{dI}{dW} = \frac{2\pi e}{\hbar} \int \left([f(E) - f(E + eW)] \frac{d}{dW} \text{Tr}[\rho_1^0(E) t^\dagger(E) \rho_2^0(E) t(E)] \right.
$$

$$
\left. - e f'(E + eW) \text{Tr}[\rho_1^0(E) t^\dagger(E) \rho_2^0(E) t(E)] \right) dE. \tag{38}
$$

Taking the limit $W \to 0$, we obtain

$$
G(0, \theta) = \frac{2\pi e^2}{\hbar} \int [-f'(E)] \text{Tr}[\rho_1^0(E) t^\dagger(E) \rho_2^0(E) t(E)] \, dE. \tag{39}
$$

In the limit $\theta = 0$, $-f'(E)$ becomes $2\delta(E - E_F)$, with spin degeneracy, and hence

$$G(0, 0) = (4\pi e^2/\hbar) \, \text{Tr}[\rho_1^0(E_F)t^\dagger(E_F)\rho_2^0(E_F)t(E_F)] \tag{40}$$

where E_F is the Fermi energy for the coupled system in the absence of an applied voltage.

Equation (40) is a *generalization* of the Landauer conductance formula [5–10], because the derivation of (40) is based on *no* assumptions about the leads, other than that they have stationary states.

In deriving (40), we assumed that the electrochemical potential drop between the leads in the steady state is the same as that between the reservoirs, W, and in defining G we took the derivative of I with respect to W. Now, it is well known [5–10] that, in general, charge neutrality in the leads requires that the electrochemical potential drop (or the rigid shift included in H_0) between the leads, W_{leads}, be given by a function of W, $F(W)$, where $F(W)$ depends on the transmission properties of the sample. Explicit expressions have been obtained [5–10] for

$$\lim_{W \to 0} (dW_{\text{leads}}/dW)$$

at $\theta = 0$ for the case of perfectly conducting leads.

If $W_{\text{leads}} \neq W$, then in defining G we have a choice between differentiating I either with respect to W or with respect to W_{leads}, leading to different results. In particular, defining G_{leads} as dI/dW_{leads}, the analogue of (40) is

$$G_{\text{leads}}(0, 0) = (4\pi e^2/\hbar) \, \text{Tr}[\rho_1^0(E_F)t^\dagger(E_F)\rho_2^0(E_F)t(E_F)]/(dW_{\text{leads}}/dW)_{W=0}. \tag{41}$$

It is worth pointing out that there is no contradiction between equations (40) and (41): both have been obtained from the same expression for the current, equation (37), and we can unambiguously go from $G(0, 0)$ to $G_{\text{leads}}(0, 0)$ and vice versa by the conversion factor $(dW_{\text{leads}}/dW)_{W=0}$. In many important cases, however, such as conduction between two semi-infinite 3D systems via a finite sample, W_{leads} will be equal to W with a unique definition of the conductance.

4. Applications

For purposes of illustration we now apply equation (40) to three physical situations: the one-atom contact, the disordered, finite 1D chain, and the generalized stacking fault. In all of them we shall use a 1-S nearest-neighbour orthonormal tight-binding (TB) model. Also, in all of them, the leads 1 and 2 will be represented by semi-infinite perfect crystals.

We shall require some preliminary results. A semi-infinite perfect crystal can be represented by a stack of 2D atomic layers, as illustrated in figure 3. Each of these layers in isolation has a set of eigenstates $\{|q\rangle\}$ with eigenvalues $\{E(q)\}$, where q is a transverse wavevector. If $|R_n\rangle$ is a 1-S orbital on the nth atom in the layer, where R_n is the position vector of the atom, then

$$|q\rangle = \frac{1}{\sqrt{N_2}} \sum_n \exp(iq \cdot R_n)|R_n\rangle \tag{42}$$

where $1/\sqrt{N_2}$ is a normalization factor. Both $\{|q\rangle\}$ and $\{|R_n\rangle\}$ are complete orthonormal sets for the layer.
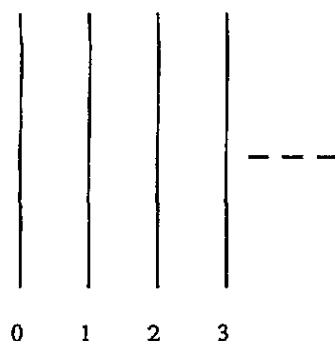
Figure 3. A semi-infinite perfect crystal, viewed as a stack of 2D atomic layers.
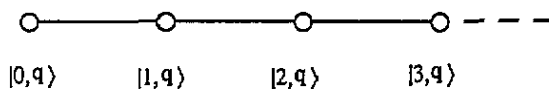
Figure 4. A semi-infinite chain of 2D states with transverse wavevector q.

Let now $|l, q\rangle$ stand for the 2D state of wavevector q on the lth layer of the crystal. $\{|l, q\rangle\}$ is an orthonormal basis for the semi-infinite crystal. Let $|R_n^l\rangle$ by a 1-S orbital on the nth atom in the lth layer, with position vector R_n^l. Then $|l, q\rangle$ is given by

$$|l, q\rangle = \frac{1}{\sqrt{N_2}} \sum_n \exp(\mathrm{i}q \cdot R_n^l)|R_n^l\rangle. \tag{43}$$

Owing to the transverse translational symmetry of the semi-infinite crystal, the eigenstates for the crystal will contain only 2D states with the same q

$$|\psi(q)\rangle = \sum_l C_l(q)|l, q\rangle \tag{44}$$

where $|\psi(q)\rangle$ is an eigenstate for the crystal with transverse wavevector q, and $\{C_l(q)\}$ are expansion coefficients.

Consequently, if $q \neq q'$, then $\langle l, q|H|m, q'\rangle$ and $\langle l, q|G^\pm|m, q'\rangle$, where H and $G^\pm$ are the Hamiltonian and the Green operators for the crystal, respectively, will be identically equal to zero for all l, m. We assume that $\langle l, q|H|m, q\rangle$ vanishes unless $m = l, l \pm 1$. When $m = l$, the matrix element becomes the on-layer energy $E(q)$. For $\langle l, q|H|l + 1, q\rangle$, we introduce the symbol $A(q)$. For $\langle l, q|G^\pm(E)|m, q\rangle$, we introduce the symbol $G_{lm}^\pm(E, q)$. We now calculate $G_{00}^+(E, q)$.

Consider a semi-infinite chain of 2D states with transverse wavevector q, as illustrated in figure 4. We can construct the above chain from the state $|0, q\rangle$ in isolation and the semi-infinite chain starting at $|1, q\rangle$ by the introduction of a perturbation H', coupling $|0, q\rangle$ to $|1, q\rangle$, as illustrated in figure 5. Let situation (a) have a Green operator G^{0+}, and situation (b) a Green operator G^+. We have

$$\langle 0, q|H'|1, q\rangle = H'_{01}(q) = A(q) \tag{45}$$

$$\langle 0, q|G^{0+}(E)|0, q\rangle = G_{00}^{0+}(E, q) = \lim_{\epsilon \to 0^+} \frac{1}{E - E(q) + \mathrm{i}\epsilon} \tag{46}$$

$$G_{00}^+(E, q) = G_{11}^{0+}(E, q). \tag{47}$$

From the Dyson equation

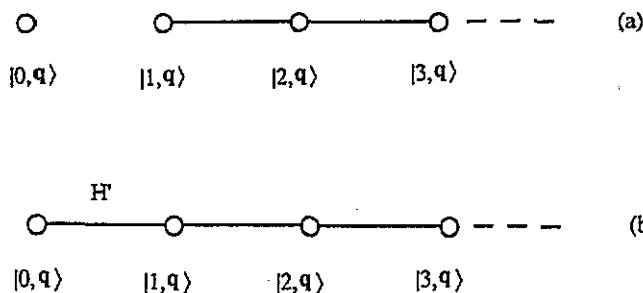$$G^+ = G^{0+} + G^{0+}H'G^+ \tag{48}$$

Figure 5. A semi-infinite chain of 2D states of transverse wavevector q and a 2D state with q in isolation (a) used to generate a new semi-infinite chain of 2D states with q (b) by the introduction of a coupling H'.
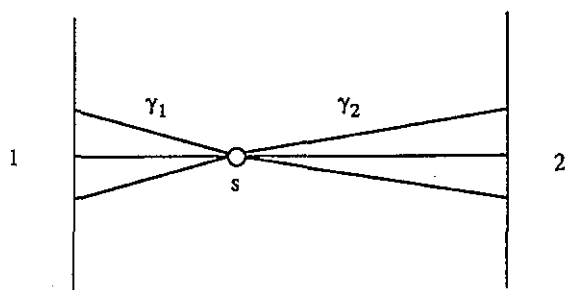

Figure 6. A single atom s between two identical semi-infinite FCC crystals 1 and 2, cut along their (1 1 1) planes. The hopping integrals between s and its three nearest neighbours in 1 are the same and equal to γ_1, and the hopping integrals between s and its three nearest neighbours in 2 are the same and equal to γ_2.

for $G_{00}^+(E, q)$ we obtain

$$G_{00}^+(E, q) = G_{00}^{0+}(E, q) + G_{00}^{0+}(E, q)H_{01}'(q)G_{11}^{0+}(E, q)H_{10}'(q)G_{00}^+(E, q)$$

which, using (45)–(47), can be solved for $G_{00}^+(E, q)$

$$G_{00}^+(E, q) = \frac{[E - E(q)] \pm \sqrt{\{[E - E(q)]^2 - 4A(q)A(q)^*\}}}{2A(q)A(q)^*} \qquad (49)$$

disregarding the special case when *both* $(E - E(q))$ and $A(q)A(q)^*$ are zero, which requires special care. Now we have to choose between the two solutions for $G_{00}^+(E, q)$.

In the case when the expression under the square root in (49) is negative, we choose the solution with the minus sign, since we want the imaginary part of $G_{00}^+(E, q)$ to be negative.

In the case when the expression under the square root is positive (so that the imaginary part of $G_{00}^+(E, q)$ is zero), we choose the solution that tends to $G_{00}^{0+}(E, q) = 1/[E - E(q)]$ as $A(q)A(q)^*$ tends to zero. In other words, we choose the plus sign if $[E - E(q)] < 0$ and the minus sign if $[E - E(q)] > 0$.

Having thus computed $G_{00}^+(E, q)$, we can now calculate the matrix element of G^+ between atomic sites m and n on the surface of the semi-infinite crystal

$$\langle R_m^0 | G^+(E) | R_n^0 \rangle = \sum_{l;l';q} \langle R_m^0 | l, q \rangle \langle l, q | G^+(E) | l', q \rangle \langle l', q | R_n^0 \rangle$$

$$= \frac{1}{N_2} \sum_q \{\exp[iq \cdot (R_m^0 - R_n^0)]\} G_{00}^+(E, q). \qquad (50)$$

But since q is a continuous label, we can replace $(1/N_2) \sum_q$ by $[\alpha/(2\pi)^2] \int d^2q$, where α depends on the geometry of the 2D layers, and the integral is taken over the first Brillouin

zone for the layer. Thus, (50) becomes

$$\langle R_m^0 | G^+(E) | R_n^0 \rangle = \frac{\alpha}{(2\pi)^2} \int \{\exp[i q \cdot (R_m^0 - R_n^0)]\} G_{00}^+(E, q) \, d^2 q. \tag{51}$$

Finally, we introduce γ as the hopping integral (matrix element of H) between nearest-neighbour atomic sites in the perfect crystal and note that, in a 1-S orbital TB mode, both H and $G^{\pm}$ are symmetric matrices in the atomic basis $\{|R_n^l\rangle\}$.

Now that we know how to calculate the matrix elements of the Green operator for a semi-infinite perfect crystal between sites on the surface in a 1-S nearest-neighbour TB model, we proceed with the three illustrative examples.

4.1. The one-atom contact

The reader will be familiar with previous TB calculations on the one-atom contact [11-13] in the context of the experiments by Gimzewski and Möller [14].

In the present calculation the sample s is a single atom and the leads 1 and 2 are identical semi-infinite perfect FCC crystals cut along their (1 1 1) planes. The atom s is between 1 and 2 and is equidistant from its three nearest neighbours on both crystal surfaces. Let $[\{|1\rangle\}, |s\rangle, \{|2\rangle\}]$ be the orthonormal atomic basis with $|1\rangle$ being a 1-S orbital in crystal 1, $|s\rangle$ being the 1-S orbital on the sample atom and $|2\rangle$ being a 1-S orbital in crystal 2. V couples s to its three nearest neighbours on the surfaces of 1 and 2. Thus, $\langle 1|V|s\rangle = \langle s|V|1\rangle = \gamma_1$ if $|1\rangle$ is the 1-S orbital on one of the three nearest neighbours of s on the surface of lead 1 and $\langle 1|V|s\rangle = \langle s|V|1\rangle = 0$ for all other $|1\rangle$). Similarly, $\langle 2|V|s\rangle = \langle s|V|2\rangle = \gamma_2$ if $|2\rangle$ is the 1-S orbital on one of the three nearest neighbours of s on the surface of lead 2 and $\langle 2|V|s\rangle = \langle s|V|2\rangle = 0$ for all other $|2\rangle$). This situation is presented diagrammatically in figure 6. Also, $\langle s|V|s\rangle = 0$.

Taking the trace in the atomic basis and remembering that $\rho_{1;2}^0 = (G_{1;2}^{0-} - G_{1;2}^{0+})/(2\pi i)$, and that $G_{1;2}^{0\pm}$ are symmetric matrices in the atomic basis, we obtain from (40)

$$G(0,0) = \frac{e^2}{\pi\hbar} 4 \sum_{1;1';2;2'} \text{Im}[\langle 1|G_1^{0+}(E_F)|1'\rangle] \, \text{Im}[\langle 2|G_2^{0+}(E_F)|2'\rangle] \gamma_1^2 \gamma_2^2 |\langle s|G^+(E_F)|s\rangle|^2 \tag{52}$$

where indices 1 and 1' run over the three nearest neighbours of s on the surface of lead 1, and similarly for indices 2 and 2' and the surface of 2. Let $|\gamma| \langle 1|G_1^{0+}(E_F)|1\rangle = g = |\gamma| \langle 2|G_2^{0+}(E_F)|2\rangle$, where $|1\rangle$ and $|2\rangle$ are sites on the surfaces of leads 1 and 2 respectively, and γ, once again, is the hopping integral between nearest neighbours in the perfect crystals. Also, let $|\gamma| \langle 1|G_1^{0+}(E_F)|1'\rangle = f = |\gamma| \langle 2|G_2^{0+}(E_F)|2'\rangle$, where $|1\rangle$, $|1'\rangle$ and $|2\rangle$, $|2'\rangle$ are pairs of nearest-neighbour sites on the surfaces of leads 1 and 2, respectively. Let $\lambda_1 = \gamma_1/|\gamma|$ and $\lambda_2 = \gamma_2/|\gamma|$. Solving the Dyson equation for $\langle s|G^+(E_F)|s\rangle$ and substituting in (52), we find

$$G(0,0) = \frac{e^2}{\pi\hbar} \frac{36[\text{Im}(g + 2f)]^2 \lambda_1^2 \lambda_2^2}{|\Delta - 3(\lambda_1^2 + \lambda_2^2)(g + 2f)|^2} \tag{53}$$

where $\Delta = E_F/|\gamma|$. The on-site energy E_0 is zero on all atoms: $E_0 = \langle 1|H|1\rangle = \langle s|H|s\rangle = \langle 2|H|2\rangle = 0$, for all 1, 2.

Since λ_1 and λ_2 depend on the distances of s from the two crystal surfaces, equation (53) enables us to compute $G(0,0)$ as a function of the position of s between the crystals. In fact, assuming all hopping integrals to be the same as those between 1-S orbitals on isolated pairs of hydrogen-like atoms, we can calculate λ_1 and λ_2 analytically:

$$\lambda_{1,2} = -\exp[(a/r_0)(1 - z_{1,2})] \frac{1 + (a/r_0)z_{1,2}}{1 + a/r_0} \tag{54}$$

where a is the nearest-neighbour separation in the crystals, r_0 is the Bohr radius of the 1-S orbital and $z_{1,2}$ are the distances of s from its nearest neighbours on surfaces 1 and 2, respectively, in units of a.

Choosing Δ to correspond to half-filled bands in the crystals, computing g and f and setting $\lambda_1 = \lambda_2 = -1$ (so that s is stably bonded to both crystal surfaces) we find a zero-voltage, zero-temperature conductance, $G(0,0)$, of 1.0 in units of $e^2/\pi\hbar$. In fact, inspection of (53) shows that $e^2/\pi\hbar$ is the maximum possible value of $G(0,0)$.

4.2. *The disordered 1D chain*

Now the sample s is a 1D atomic chain containing N atoms. The atoms in the chain are labelled as $s_1, s_2, \ldots, s_N$. The leads 1 and 2 are once again identical semi-infinite perfect FCC crystals cut along their (1 1 1) planes. V couples s_1 to its three nearest neighbours on the surface of lead 1, and s_N to its three nearest neighbours on the surface of lead 2. We imagine s_1 to be stably bonded to crystal 1 and s_N to be stably bonded to crystal 2. In other words, if $[\{|1\rangle\}, \{|s_n\rangle\}, \{|2\rangle\}]$ is the orthonormal atomic basis, then $\langle 1|V|s_1\rangle = \langle s_1|V|1\rangle = \langle 2|V|s_N\rangle = \langle s_N|V|2\rangle = \gamma$ if $|1\rangle$ and $|2\rangle$ are among the respective groups of nearest neighbours of s. All other matrix elements of V are zero. This situation is presented in figure 7.
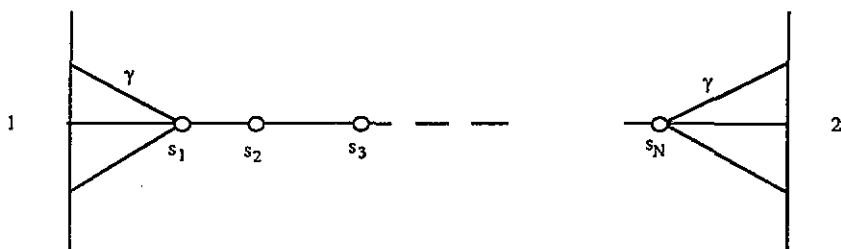

Figure 7. A 1D chain of N atoms, $s_1, s_2, \ldots, s_N$, between two identical semi-infinite FCC crystals 1 and 2, cut along their (1 1 1) planes; s_1 is stably bonded to the surface of 1 and s_N is stably bonded to the surface of 2.

Taking the trace in the atomic basis, and employing the same definition of g and f as before, we obtain from (40)

$$G(0,0) = (e^2/\pi\hbar)36[\text{Im}(g+2f)]^2|\langle s_1|G^+(E_F)|s_N\rangle|^2|\gamma|^2. \tag{55}$$

Solving the Dyson equation for $\langle s_1|G^+(E_F)|s_N\rangle$, we get

$$|\gamma|\langle s_1|G^+(E_F)|s_N\rangle = |\gamma|\langle s_1|G^{0+}(E_F)|s_N\rangle\{1 - 3(g+2f)|\gamma|[\langle s_1|G^{0+}(E_F)|s_1\rangle$$
$$+ \langle s_N|G^{0+}(E_F)|s_N\rangle] + 9(g+2f)^2|\gamma|^2[\langle s_1|G^{0+}(E_F)|s_1\rangle\langle s_N|G^{0+}(E_F)|s_N\rangle$$
$$- \langle s_1|G^{0+}(E_F)|s_N\rangle^2]\}^{-1}. \tag{56}$$

We introduce the notation $B_{bb}(n)/|\gamma|$ for the on-site matrix element of the (+) Green operator on the first site ('b' stands for 'beginning') of a 1D chain of length n atoms, $B_{be}(n)/|\gamma|$ for the matrix element of the (+) Green operator between the first and the last sites ('e' stands for 'end') of a 1D chain of length n, and $B_{ee}(n)/|\gamma|$ for the on-site matrix

element of the (+) Green operator on the last site of a 1D chain of length n, at E_F. Thus, for the complete chain we have

$$|\gamma|\langle s_1|G^{0+}(E_F)|s_1\rangle = B_{bb}(N)$$

$$|\gamma|\langle s_1|G^{0+}(E_F)|s_N\rangle = B_{be}(N)$$

$$|\gamma|\langle s_N|G^{0+}(E_F)|s_N\rangle = B_{ee}(N).$$

Suppose we construct the complete chain starting from a single atom, s_1, and adding the rest, s_2, s_3, etc, one at a time. Let the coupling of s_n to s_{n-1} by $\lambda(n)$ in units of $|\gamma|$. Let the on-site energy on s_n be $\epsilon(n)$ in units of $|\gamma|$. Then, solving the Dyson equation at each step, we obtain the iterative equations

$$B_{ee}(n) = 1/[\Delta - \epsilon(n) - \lambda(n)^2 B_{ee}(n-1)] \tag{57}$$

$$B_{be}(n) = B_{be}(n-1)\lambda(n)B_{ee}(n) \tag{58}$$

$$B_{bb}(n) = B_{bb}(n-1) + B_{be}(n-1)\lambda(n)B_{be}(n) \tag{59}$$

where, once again, $\Delta = E_F/|\gamma|$. Starting with $B_{ee}(1) = B_{be}(1) = B_{bb}(1) = 1/\Delta$, we can calculate $B_{ee}(N)$, $B_{be}(N)$ and $B_{bb}(N)$ from equations (57)–(59). Hence, from (56) we obtain $|\gamma|\langle s_1|G^+(E_F)|s_N\rangle$ and hence, from (55), $G(0,0)$. The value of Δ is chosen to correspond to half-filled bands in the crystals.

First, we look at the perfect chain, defined by $\lambda(n) = -1, \epsilon(n) = \epsilon$, for all n. Computation shows that, when the chain is made of the same atoms as the crystals, i.e. $\epsilon = 0$, $G(0,0)$ remains equal to 1.0 in units of $e^2/\pi\hbar$ for any value of N. (We have studied the case $N \leqslant 10\,000$.) $G(0,0) \leqslant 1.0e^2/\pi\hbar$ for all other values of ϵ. In particular, for $\epsilon > \Delta + 2$ or $\epsilon < \Delta - 2$, $G(0,0)$ is essentially zero for $N \gtrsim 30$. The reason for this is that the band for the perfect chain lies in the energy range $[\epsilon - 2, \epsilon + 2]$ and if $\epsilon > \Delta + 2$ or $\epsilon < \Delta - 2$, then there are no eigenstates for the chain at E_F.

Now we investigate the disordered chain. We shall consider three types of disorder: (i) pure positional, with $\lambda(n)$ being a random variable and $\epsilon(n)$ being constant; (ii) pure compositional, with $\lambda(n)$ being constant and $\epsilon(n)$ being a random variable; and (iii) combined, with both $\lambda(n)$ and $\epsilon(n)$ being random variables. In all three cases, we want to study $G(0,0)$ as a function of N. In our simulations we use a random number generator, $\text{ran}(x)$, to generate random reals in the interval $[0, 1)$.

For producing disorder (i), we use

$$\lambda(n) = -[0.5 + 0.5\,\text{ran}(x)] \tag{60}$$

to generate a rectangular distribution for $\lambda(n)$ with $-\lambda(n) \in [0.5, 1)$. Also, we set $\epsilon(n) = 0$, for all n.

For disorder (ii), we use

$$\epsilon(n) = 1 - 2\,\text{ran}(x) \tag{61}$$

to produce a rectangular distribution for $\epsilon(n)$ with $\epsilon(n) \in (-1, 1]$, and set $\lambda(n) = -1$, for all n.

For disorder (iii), we use generating procedures (60) and (61) in conjunction with each other.

In all three cases, $G(0,0)$ exhibits extremely unstable behaviour with respect to the random configuration. In fact, for a fixed N, $G(0,0)$ may vary by several orders
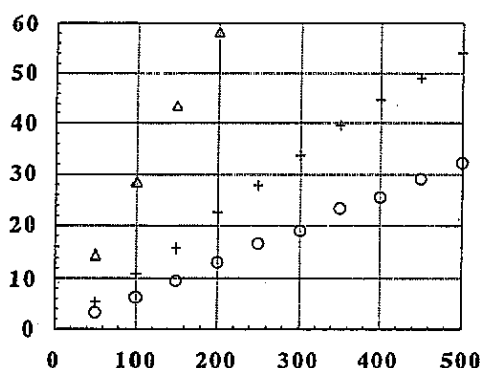
Figure 8. Plot of $\langle -\ln G(0,0)\rangle$ (vertical axis) versus N (horizontal axis) for various types of disorder in a 1D chain of length N. (O) Case (i), pure positional disorder with $-\lambda(n) \in [0.5, 1)$ and $\epsilon(n) = 0$, for all n. (+) Case (ii), pure compositional disorder with $\lambda(n) = -1$, for all n, and $\epsilon(n) \in (-1, 1]$. (△) Case (iii), combined disorder with $-\lambda(n) \in [0.5, 1)$ and $\epsilon(n) \in (-1, 1]$. $G(0, 0)$ is in units of $e^2/\pi\hbar$.
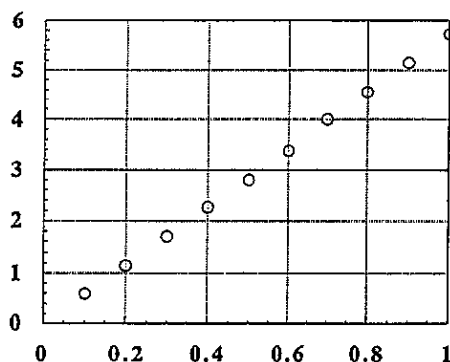
Figure 9. Plot of $[\langle -\ln G(0,0)\rangle]^{1/2}$ (vertical axis) versus u (horizontal axis) for varying pure compositional disorder in a 1D chain of length $N = 300$, with $\epsilon(n) \in (-u, u]$, $\langle \epsilon(n)\rangle = 0$ and $\sigma[\epsilon(n)] \sim u, \lambda(n) = -1$, for all n. $G(0, 0)$ is in units of $e^2/\pi\hbar$.

of magnitude with the random configuration. We are, therefore, compelled to use configurational averages.

We have computed $\langle -\ln G(0, 0)\rangle$, where the average is taken over 200 configurations and $G(0, 0)$ is in units of $e^2/\pi\hbar$, as a function of N. The results are presented in figure 8. The straightness of the lines demonstrates the exponential spatial localization of the carriers in the disordered 1D region.

Next, we look at the dependence of $G(0, 0)$ on the *extent* of the disorder for a fixed N. We consider two cases: (iv) varying pure compositional disorder, and (v) varying pure positional disorder.

For (iv) we use

$$\epsilon(n) = u[1 - 2\operatorname{ran}(x)] \tag{62}$$

producing a rectangular distribution for $\epsilon(n)$ with $\epsilon(n) \in (-u, u]$, $\langle \epsilon(n)\rangle = 0$ and $\sigma[\epsilon(n)] \sim u$, where σ stands for standard deviation. We set $\lambda(n) = -1$, for all n. In figure 9 we have plotted $[\langle -\ln G(0, 0)\rangle]^{1/2}$ versus u for $N = 300$, where the averages of $-\ln G(0, 0)$ are taken over 500 configurations, and $G(0, 0)$ is in units of $e^2/\pi\hbar$. The results suggest that $G(0, 0)$ decreases exponentially with the variance, σ^2, of $\epsilon(n)$ for a fixed N.

For (v) we use

$$\lambda(n) = -[1 - u\operatorname{ran}(x)] \tag{63}$$

producing a rectangular distribution for $\lambda(n)$ with $-\lambda(n) \in (1 - u, 1]$, $\langle -\lambda(n)\rangle = 1 - u/2$ and $\sigma[\lambda(n)] \sim u$. We set $\epsilon(n) = 0$, for all n. In figure 10 we have plotted $(1 - u/2)[\langle -\ln G(0, 0)\rangle]^{1/2}$ versus u for $N = 300$, where, once again, the averages of $-\ln G(0, 0)$ are taken over 500 configurations, and $G(0, 0)$ is in units of $e^2/\pi\hbar$. The results suggest that for small $\sigma[\lambda(n)]$, $G(0, 0)$ decreases exponentially with $\sigma^2[\lambda(n)]/\langle \lambda(n)\rangle^2$ for a fixed N.
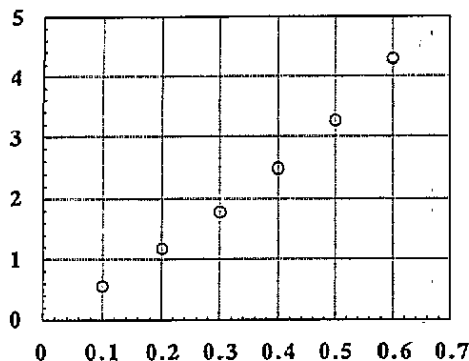
Figure 10. Plot of $(1-u/2)[\{-\ln G(0,0)\}]^{1/2}$ (vertical axis) versus u (horizontal axis) for varying pure positional disorder with $-\lambda(n) \in (1-u, 1]$, $\langle -\lambda(n) \rangle = 1 - u/2$ and $\sigma[\lambda(n)] \sim u$, $\epsilon(n) = 0$, for all n, in a 1D chain of length $N = 300$. $G(0,0)$ is in units of $e^2/\pi\hbar$.
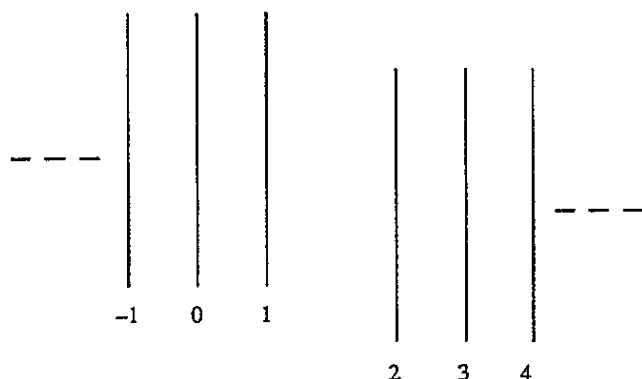

Figure 11. Two semi-infinite crystals, shifted relative to each other along the interface between them.

4.3. The generalized stacking fault

In this example there is no sample. In other words, the leads 1 and 2 are coupled directly to each other. The leads are again identical, semi-infinite perfect FCC crystals, cut along their (1 1 1) planes, shifted relative to each other along the (1 1 1) planes by an arbitrary amount. Again, the crystals can be thought of as stacks of 2D atomic layers. We label these layers by an integer $n \in (-\infty, +\infty)$, so that all layers with $n \leqslant 1$ belong to lead 1 and all layers with $n \geqslant 2$ belong to lead 2 (figure 11).
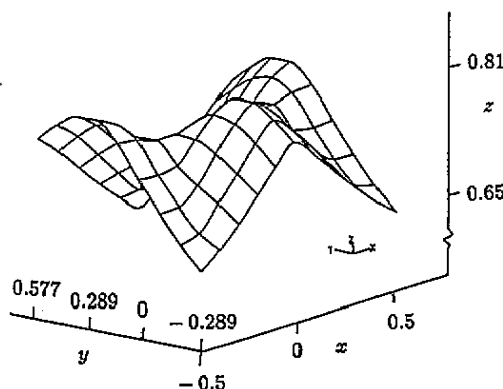

Figure 12. Conductance per atom (z axis) versus relative displacement (xy plane) of two identical semi-infinite FCC crystals, cut along their (1 1 1) planes. The x axis is the displacement along $[0\,1\,\bar{1}]$ in units of the nearest-neighbour separation a in the perfect crystal, and the y axis is the displacement along $[\bar{2}\,1\,1]$ in units of a.

We shall employ the orthonormal basis $\{|l, \boldsymbol{q}\rangle\}$, where, again, $|l, \boldsymbol{q}\rangle$ is a 2D eigenstate of

wavevector q in the lth layer. V couples each atom in layer 1 to its three nearest neighbours in layer 2. Since V does not disturb the transverse translational symmetry of the system, H and $G^{\pm}$ are diagonal in q, i.e. if $q \neq q'$, then $\langle l, q|H|m, q'\rangle$ and $\langle l, q|G^{\pm}|m, q'\rangle$ vanish identically for all l, m. Thus, the only non-zero matrix elements of V are $\langle 1, q|V|2, q\rangle$ and $\langle 2, q|V|1, q\rangle$. Taking the trace in the basis $\{|l, q\rangle\}$, we obtain from (40)

$$G(0, 0) = \frac{e^2}{\pi\hbar} 4 \sum_q \left\{ \mathrm{Im}[G_{11}^{0+}(E_\mathrm{F}, q)] \right\}^2 |t_{21}(E_\mathrm{F}, q)|^2 \tag{64}$$

where we have used the fact that $G_{11}^{0+}(E_\mathrm{F}, q) = G_{22}^{0+}(E_\mathrm{F}, q)$. Solving the Dyson equation

$$t = V + VG^{0+}t \tag{65}$$

for $t_{21}(E_\mathrm{F}, q)$, substituting in (64), dividing (64) by N_2 to obtain the conductance per atom in the interface and replacing $(1/N_2) \sum_q$ by $[\alpha/(2\pi)^2] \int \mathrm{d}^2q$, we find

$$\frac{1}{N_2} G(0, 0) = \frac{e^2}{\pi\hbar} \frac{4\alpha}{(2\pi)^2} \int \frac{\{\mathrm{Im}[G_{11}^{0+}(E_\mathrm{F}, q)]\}^2 |V_{21}(q)|^2}{|1 - [G_{11}^{0+}(E_\mathrm{F}, q)]^2 |V_{21}(q)|^2|^2} \mathrm{d}^2q. \tag{66}$$

E_F is again chosen to correspond to half-filled bands in the crystals. The separation of crystals 1 and 2 is chosen in such a way that the distance between each atom in layer 1 and its nearest neighbour in layer 2 remains constant and equal to the nearest-neighbour separation a in the crystals. For the hopping integrals between atoms in layer 1 and their nearest neighbours in layer 2, we use the scaling law, specified in equation (54).

Computation of (66) shows that $G(0, 0)/N_2$ has a maximum when the two semi-infinite crystals are stably bonded (so as to form one infinite perfect crystal), i.e. when $V_{12}(q) = A(q)$, and has a minimum when the two crystals are displaced in such a way that each atom in layer 1 is directly opposite an atom in layer 2. The maximum conductance is $0.81e^2/\pi\hbar$ per atom. This result is direct evidence for quantum interference. In the one-atom contact calculation, we found a conductance of $1.0e^2/\pi\hbar$ when the single atom was stably bonded to both crystal surfaces. If the conductance were simply proportional to the number of one-atom contacts between the two crystals, then the maximum conductance per atom in the stacking fault calculation would also be $1.0e^2/\pi\hbar$. The fact that it is not means that there is interference between the different one-atom contacts, making up the interface between 1 and 2. $G(0, 0)/N_2$ for all other stacking fault configurations depends on a/r_0, where r_0 is the Bohr radius of the 1-S orbital. With $a/r_0 = 2$, we find a minimum conductance per atom of $0.65e^2/\pi\hbar$, yielding a contrast of about 20%. In figure 12 we have plotted the conductance per atom, $G(0, 0)/N_2$, in units of $e^2/\pi\hbar$ as a function of the displacement of crystal 2 relative to crystal 1 with $a/r_0 = 2$.

5. Summary

In conclusion, we may say that we have at our disposal a methodology with the aid of which the computation of the elastic conductance of a wide range of structures becomes easy. The results of the analysis emphasize the point that in elastic transport the conductance of a circuit, containing a sample, is determined by the coupling of the sample to the other components of the circuit, and by the nature of these components, as well as by the sample itself. The method can be extended to include self-consistency corrections to the non-interacting single-particle states $\{|\psi_n^+\rangle\}$, or, equivalently, to the matrix elements of $G^{\pm}$ by

solving the Lippmann–Schwinger or the Dyson equations, respectively, with some self-consistent field potential.

The results of this work will be applied in the future to the study of the conduction properties of the tip–surface contact both in the tunnelling and in the contact regimes for the scanning tunnelling microscope (STM). This study will be based on the molecular dynamics simulations research conducted at this department [15].

References

[1]   Merzbacher E 1961 *Quantum Mechanics* (Chichester: Wiley) section 21.8
       Roman P 1965 *Advanced Quantum Theory* (Reading, MA: Addison-Wesley) section 4.4
[2]   Pendry J B, Pretre A B and Krutzen B C H 1991 *J. Phys.: Condens. Matter* **3** 4313
[3]   Meir Y and Wingreen N S 1992 *Phys. Rev. Lett.* **68** 2512
[4]   Bardeen J 1961 *Phys. Rev. Lett.* **6** 57
[5]   Anderson P W, Thouless D J, Abrahams E and Fisher P S 1980 *Phys. Rev.* B **22** 3519
[6]   Azbel M Ya 1980 *Phys. Lett.* **78A** 410
[7]   Azbel M Ya 1981 *J. Phys. C: Solid State Phys.* **14** L225
[8]   Büttiker M, Imry Y, Landauer R and Pinhas S 1985 *Phys. Rev.* B **31** 6207
[9]   Payne M C 1989 *J. Phys.: Condens. Matter* **1** 4931
[10]   Landauer R 1989 *J. Phys.: Condens. Matter* **1** 8099
[11]   Martin-Rodero A and Flores F 1988 *Phys. Rev.* B **38** 10 047
[12]   Ferrer J, Martin-Rodero A and Flores F 1988 *Phys. Rev.* B **38** 10 113
[13]   Martin-Rodero A, Ferrer J and Flores F 1988 *J. Microsc.* **152** 317
[14]   Gimzewski J K and Möller R 1987 *Phys. Rev.* B **36** 1284
[15]   Sutton A P and Pethica J B 1990 *J. Phys.: Condens. Matter* **2** 5317